Research Article

Received: 15 December 2017 Revised: 1 February 2018 Accepted article published: 13 April 2018 Published online in Wiley Online Library: 21 May 2018

(wileyonlinelibrary.com) DOI 10.1002/pi.5610

Shape memory composites based on a thermoplastic elastomer polyethylene with carbon nanostructures stimulated by heat and solar radiation having piezoresistive behavior

Humberto Palza,[a*] Paula Zapata[b] and Christian Sagredo[a]

Abstract

A thermoplastic elastomer polyethylene (TEPE) based on an ethylene/1-butene copolymer having shape memory effect (SME) without any chemical modification is presented and the effect of adding either carbon nanotubes or thermally reduced graphite oxide is analyzed. For electrical percolated samples, the development of a polymer sensor that changes its electrical conductivity under solar radiation triggered by SME is further presented. Our results showed that programmed samples recovered their permanent shape showing SME under a direct heating stimulus at 60 °C. The addition of carbon nanostructures increased the times needed to reach 100% recovery as compared with pure TEPE. Noteworthy, the SME was also stimulated remotely by solar radiation increasing the sample temperature. Composites presented a faster SME under this remote radiation process as compared with pure TEPE due to their higher radiation absorption. Percolated TEPE/carbon nanotube composites displayed further a decrease in the electrical resistivity during SME under this solar radiation. Finally, our results showed that the glass transition also triggered the SME in these samples allowing the development of triple shape memory polyethylenes without any chemical crosslinking process. Based on these findings, a simple route was developed to produce double, or even triple, shape memory piezoresistive polyethylenes that can be activated remotely by solar radiation.

Keywords: polymer composites; nanocomposites; smart polymers

INTRODUCTION

Shape memory polymers (SMPs) are stimuli-responsive smart materials able to undergo a large/macroscopic recoverable deformation upon the application of an external stimulus. They can therefore change from a temporary shape to their original (or permanent) shape under a stimulus such as temperature, light, electric field, magnetic field, pH, specific ions or enzymes.[1] The shape memory effect (SME) is not an intrinsic property, meaning that polymers do not display this effect by themselves, and it results from a combination of polymer morphology and specific processing.[2] SMPs are elastic polymer networks having both reversible stimuli-sensitive molecular switches and net-points (irreversible during the whole process), the latter determining the permanent shape by chemical or physical interactions.[2] In polymers, SME needs at least two separated phases such as in physical crosslinking polymers whose morphology consists of segregated domains.[3] A domain with a specific thermal transition temperature (T_{trans}) can act as a molecular switch having flexibility and entropic elastic behavior above this transition. When the sample is externally stressed from its permanent shape at a temperature $T > T_{trans}$, forming the temporary shape, the deformed chain segments should be prevented from recoiling through reversible molecular switches occurring at $T < T_{trans}$, a process called programming.[2] Upon exposure to a specific stimulus increasing the sample to $T > T_{trans}$, the switching is triggered, and the strain energy stored in the temporary shape is released, which consequently results in the shape recovery.[3] The shape recovery in SMPs is driven by the entropy elasticity of the switching segments.[4]

SMPs with switching domains thermally induced by melting, a liquid crystalline phase or glass transitions are some of the most investigated.[4] In these SMPs, the thermal response can be triggered not only by direct heating but also by electric, magnetic or electromagnetic indirect heating.[5] In particular, physically crosslinked SMPs are highlighted as they are mainly thermoplastics exhibiting a reversible nature and being able to melt or dissolve in certain solutions.[3] In amorphous thermoplastics, SME arises from the glass transition (T_g) as a deformed shape obtained at $T > T_g$ is maintained by cooling below the glassy state.[6] The permanent shape of the network is provided by physical crosslinking of polymers through molecular interactions such as van der Waals forces, dipole–dipole interactions or hydrogen bonding.[6] In semicrystalline thermoplastic materials, the existence

* *Correspondence to: H Palza, Departamento de Ingeniería Química y Biotecnología, Facultad de Ciencias Físicas y Matemáticas, Universidad de Chile, Beauchef 851, Santiago, Chile. E-mail: hpalza@ing.uchile.cl*

a *Departamento de Ingeniería Química y Biotecnología, Facultad de Ciencias Físicas y Matemáticas, Universidad de Chile, Santiago, Chile*

b *Grupo Polímeros, Facultad de Química y Biología, Universidad de Santiago de Chile, Santiago, Chile*

of two thermal transitions allows more flexibility as the polymer crystals can be either the switch segments or the net-points. From the material point of view, several polymers have been used in thermally induced physically crosslinked SMPs, mainly copolymers such as those based on polyurethane,[5–9] poly(ether ester),[10] poly(ethylene oxide)/poly(ethylene terephthalate),[11] poly(1,4-butadiene)/polystyrene,[12] polyethylene/nylon,[13] poly(*p*-dioxanone)/polycaprolactone[14] and perfluorosulfonic acid ionomer.[15] Thermoplastic homopolymers can also be thermally activated although most of them are chemically crosslinked.[16,17] During the last few years, biodegradable polymers have emerged for SPMs such as poly(L,D-lactide),[18] and its various blends,[19,20] among others.[21]

Polyolefins, in particular polyethylene (PE), are widely used in an extremely broad range of applications accounting for more than 50% by weight of the polymers produced and remaining at the top of the global production of synthetic polymers.[22] Regarding SMPs, most reports focused on partially crosslinked PE produced by irradiation allowing, for instance, the development of commercial heat-shrinkable products.[23] PE crystals are formed by cooling below the crystallization temperature defining the temporary shape by acting as physical net-points. Heating the material above the melting temperature results in the material returning to its permanent shape fixed during the irradiation process.[23] Various PE topologies have been studied for SMPs including high-density PE,[23] low-density PE,[16] ultrahigh-molecular-weight PE[24] and ethylene/1-octene copolymers.[25,26] Recently, the focus has been on triple SMPs consisting of crosslinked PE blends with polypropylene and various PEs.[27–29] Studies of polyolefins with SME based on physical crosslinking have not been reported despite the possibility of designing PE materials with controlled morphologies including thermoplastic elastomer PE with hard (bundled crystals) and soft (amorphous phase) segments, both needed for SMPs.[30]

Compared with other shape memory materials, SMPs exhibits poorer mechanical behavior limiting their use in some applications, and the incorporation of reinforcing fillers has been investigated in order to overcome this limitation.[5] Noteworthy, the addition of functional fillers into SMPs allows the thermal transition be triggered by other external stimuli such as electrical resistive heating, light or magnetic field.[3] Of the various functional fillers that can be added, carbon nanotubes (CNTs) are highlighted due to their exceptional mechanical behavior and high aspect ratios, improving the SME in SMPs.[1] CNTs can further add other functionalities to a resulting SMP composite such as electrical conductivity by a percolation process, or infrared absorption.[1] In the former case, the current passing through the composite can induce Joule heating raising the internal temperature of SMPs to above the switch transition temperature.[1] For instance, several percolated SMP/CNT composites presented electro-induced shape recovery avoiding external heating.[3,31–33] Moreover, CNTs dispersed in a thermoplastic elastomer not only increased the strain set and stored energy density but also allowed remote actuation by infrared absorption and electronic conductivity.[34] The presence of CNTs creates a cooperative physical network comprising crystalline polymer-bridging CNTs, which enables greater strain energy storage through decreased relaxation and entropic recoiling of the chains.[34] By using a polydimethylsiloxane matrix with CNTs, a mechanical response to infrared irradiation was observed depending on the external uniaxial strain applied and therefore on the particle orientation.[35] This process was explained by an infrared-photon absorption mechanism heating the composite. Chemically crosslinked ethylene/1-octene copolymers (PE thermoplastic elastomer), either alone or blended with ethylene/propylene diene rubber, were filled with carbon black to produce SMPs electrically activated by means of the Joule effect.[36,37] A thermoplastic elastomer PE (TEPE) filled with CNTs for SMPs has not been reported.

The novel actuation approaches emerging from polymer composites with functional nanoparticles can be used to develop multifunctional SMPs sensitive to a particular stimulus for sensor or actuator applications.[3] For instance, electrically conductive SMP composites filled with carbon particles could be used as strain sensors, the principle of which is based on the relation between electrical conductivity and strain (piezoresistivity). The real-time deformation of these SMP composites could be monitored by measuring the evolution of conductivity when they recover their original shape.[3] For instance, if light-induced SMPs are exposed to light of a particular wavelength, the deformation triggered would enable their use as both sensors and actuators.[3] Although copolymers having SME or polymer/CNT composites having piezoresistivity are well known, reports about SMPs with strain sensor characteristics are rare.

The goal of the work presented in this contribution was to study the double and triple SME in a commercial thermoplastic elastomer ethylene/1-butene copolymer filled with CNTs without any chemical crosslinking process. Moreover, motivated by the increasing use of graphene-based fillers in polymer nanocomposites, thermally reduced graphene oxide was also used. Our results show that these composites display SME triggered thermally by either direct heating in an oven or a remote process under solar radiation. Noteworthy, based on previous results regarding the piezoresistivity behavior of these materials,[38] we report for the first time the development of a polymer sensor that changes its electrical conductivity under solar radiation triggered by the SME, opening novel applications of these SMPs in active solar radiation sensors.

EXPERIMENTAL

Materials

A commercial ethylene/1-butene copolymer from Dow Chemical (USA) was used as the polymer matrix (ENGAGE HM 7487). Based on the datasheet information provided, the density, the total crystallinity, the melting temperature and the glass transition temperature were 0.86 g cm^{-3}, 13%, 37 °C and −57 °C, respectively. Baytubes C150P multiwall CNTs were obtained from Bayer Material Science AG (Germany). Based on the datasheet information provided, they were characterized by a purity higher than 95 wt%, number of walls between 2 and 15, an outer mean diameter of 13–16 nm, an inner mean diameter of 4 nm, a length between 1 and > 10 μm and a bulk density around 150 kg m^{-3}. CNTs were used without any purification process. Extra-pure graphite powders (G), sulfuric acid (H_2SO_4, 98.08%), potassium permanganate ($KMnO_4$, 99%), hydrochloric acid (HCl, 32%) and sodium nitrate ($NaNO_3$, 99.5%) were obtained from Merck (Germany) and used as received. Hydrogen peroxide (H_2O_2, 5%) was purchased from Kadus SA.

Thermally reduced graphite oxide (TrGO) was prepared in a two-step oxidation/thermal reduction process using G as raw material based on the process of Hummers and Offeman.[39] The first step is oxidation of G with $KMnO_4$ and $NaNO_3$ in concentrated sulfuric acid, affording graphite oxide (GO). In a second step, the dry GO was thermally reduced to afford TrGO in a nitrogen atmosphere by rapidly heating GO up to 600 °C

during 40 s using a quartz reactor heated in a vertical tube furnace.

Composite preparation and characterization

The composites were prepared by using a Brabender Plasticorder (Brabender, Germany) internal mixer at 110 °C and a speed of 110 rpm. Filler content ranged from 0 to 14 wt%. First, half of the polymer pellets were added to the mixer operated at 110 rpm. After 2 min approximately for melting the polymer, the filler was added during 3 min. Finally, the rest of polymer pellets were added and the speed of the mixer was held at 110 rpm for 10 min. Therefore, the total mixing time was around 15 min. Afterwards, the samples were press-molded at 110 °C at 50 bar for 5 min and cooled under pressure by flushing the press with cold water, in order to obtain the final samples for tests. For mechanical characterization, the samples were cut with a stainless steel mold with dimensions according to type IV (ASTM D638) with a thickness of 1 mm. After sample preparation, the materials were left at room temperature for at least 3 days allowing crystallization of the highly amorphous polymer by annealing.

The mechanical properties were measured using an HP D500 tensile test dynamometer at a rate of 50 mm min^{-1} at 23 °C and 30% relative humidity. A minimum of three samples were tested for each material and the average values are reported. The experimental error was about 6% relative to the mean value.

For the electric resistivity/conductivity, different meghommeters (Megger BM11 with a highest voltage of 1200 V and AEMC 1060 with a highest voltage of 5000 V) were used depending on the conductivity of the samples. With this setup, the standard two-point method was used. In this case, the electrodes were embedded into the samples for a bulk measurement. For each electrical value reported in this contribution, at least five samples were prepared and five measurements for each one were carried out. In general, differences around one order of magnitude were detected in the non-percolated samples having low conductivity values (*ca* 10^{-9} S cm^{-1}). For percolated samples, the experimental error for conductivities was less than 50%.

The melting behavior of the samples was investigated using a Mettler Toledo DSC1/500 differential scanning calorimeter under N_2 atmosphere to minimize thermal degradation. The samples were heated from 25 to 200 °C at a heating rate of 10 °C min^{-1}. For crystallinity measurements, the heat of fusion of completely crystalline polyethylene was assumed to be 293 J g^{-1}. An FEI field emission SEM instrument (QUANTA FEG 250) was used to analyze the filler distribution in the composites.

Characterization of the shape memory behavior in bending tests

Samples having dimensions of $90 \times 20 \times 1$ mm^3 ($l \times w \times d$) were prepared for shape memory experiments performed in bending mode. The permanent shape was associated with the rectangle in a flat shape. For the temporary shape, the samples were bent to a storage angle θ_0 by putting the sample into a U-like mold in the soft rubbery state (room temperature). The bent samples were then inserted into an oven, which was heated to the programming temperature of 60 °C. After 10 min of annealing, the samples were quenched in liquid nitrogen at around −195 °C to fix their shape. After 10 min the samples were located at room temperature. Using this procedure, U-like shaped samples were obtained and they were ready for subsequent shape memory experiments.

For thermally stimulated shape memory experiments, the programmed samples were inserted into a pre-heated oven at 60 °C. For solar radiation-stimulated shape memory experiments, the programmed samples were positioned under a solar simulator lamp (1.1 Sun), at 6 cm from the sample (Sciencetech model SF150 with a 50–300 W xenon lamp). Photographs of the samples were taken during the recovery time.

In order to quantify the recovery during SME, the shape recovery ratio (r) was defined based on the change of the contour of the sample during heating:

$$r = \frac{\theta_N - \theta_0}{180 - \theta_0} \times 100\% \quad (1)$$

where θ_0 is the initial angle determined after programming, which characterizes the ability of the composite to fix the temporary shape of the sample, and θ_N is the angle describing the recovery process during heating. A 100% recovery is reached when θ_N reaches 180°.

For piezoresistive tests under simulated solar radiation, an Arduino Uno microcontroller-based kit was used. Arduino Uno is an open source microcontroller for building digital devices and interactive objects for sensing and controlling. In our case, Arduino allowed the measurement of the electrical conductivity by programing the microcontroller and by constructing a series electrical circuit between the Arduino, the sensor (the composite) and a known electrical resistance, applying 5 V. In this way, the sensor was placed under the solar simulator lamp, and the electrical connections were located at the extreme of the sample by clamps serving as electrodes. This configuration using a surface contact is the standard for strain sensors based on polymer composites.[40] This system allowed the on-line measurement of the electrical conductivity in the recovery process under simulated solar radiation. For each composite, three samples were tested. In a similar system, electrodes deposited on the cut edges of the specimen gave the same resistivity as electrodes applied on the surfaces.[41] However, in our case, the electrical values from this configuration were much higher than results based on bulk measurements; therefore the electrical conductivity is likely by the surface. The values reported are the relative resistance defined as the ratio between the electrical resistance of the strained sample and the original resistance at permanent relaxed state.

RESULTS

Polymer characterization

Figure 1 shows the effect of adding carbon nanoparticles to TEPE on both the elastic modulus and the elongation at break. As expected for a matrix with low stiffness (elastic modulus of 3.5 MPa) as compared with more crystalline PE, the impact of nanoparticles was relevant with increases as high as 440% in the Young's modulus. Similar results, or even with greater improvements, can be obtained in other elastomeric matrices filled with carbon nanostructures such as polyurethane and poly(vinyl alcohol).[42–44] However, all these elastomers present some polarity facilitating the filler–matrix interaction in contrast with TEPE having nonpolar characteristics. The improvement is associated with the high reinforcement effect of nanoparticles on the soft polymer matrix as concluded by analyzing micromechanical models.[45] These models predicted the highest improvements in the elastic modulus of matrices with stiffness lower than 100 MPa as in our case. The final reinforcement depended on the type of

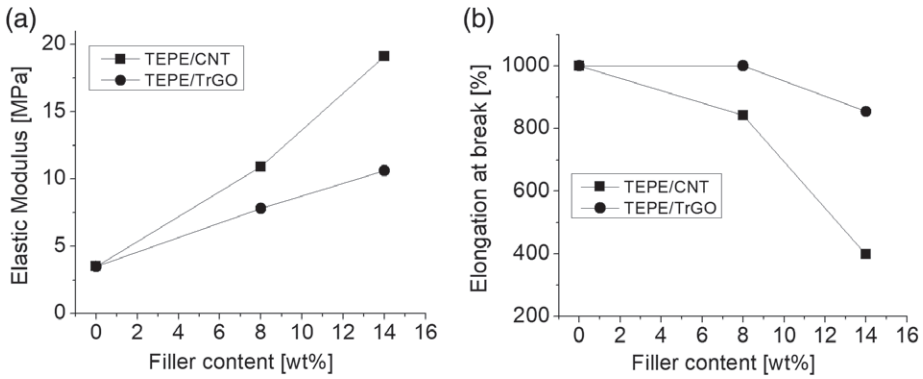

Figure 1. Effect of addition of carbon nanoparticles on the tensile mechanical behavior of TEPE: (a) elastic modulus; (b) elongation at break. For the latter property, some samples did not present a break in our strain–stress tests, and the value reported (1000%) is the maximum strain measured in the equipment.

filler, with CNTs rendering higher values than TrGO particles. In this case, the particle/agglomerate aspect ratio is one of the main variables, meaning that in our case CNTs or their agglomerates presented higher aspect ratio than TrGO fillers. TEPE can support large deformations under tensile tests, and some samples did not show any break for the conditions of our experiments, and the values reported in Fig. 1(b) corresponded to the maximum strain carried out during the test (1000%). However, a reduction in the elongation at break of some composites was observed as compared with the pure matrix, as previously reported for either CNT- or TrGO-filled polymeric composites.[44–46] Both the restrictions of polymer movements due to the particles and the premature failure starting at the particle aggregates seem to explain this tendency.[43] However, the composites still present large elongation before break.

Figure 2 displays the electrical conductivity of the various composites as a function of the filler content showing the large effect of carbon nanoparticles. When CNTs were used as filler at concentrations above 8 wt%, TEPE composites displayed a marked increase of several orders of magnitude in the conductivity. This increase means a percolation process coming from the formation of a three-dimensional network of CNTs throughout the polymer matrix. TrGO fillers in contrast were not able to render a percolation transition at similar concentrations confirming the lower aspect ratio coming from their agglomeration as compared with CNTs. The latter is based on the inverse relationship between particle aspect ratio and percolation threshold.[47] Figure 3 displays SEM images of representative composites with CNTs and TrGO confirming the different aspect ratios between the fillers. While CNTs were dispersed throughout the polymer matrix with isolated particles having high aspect ratio, TrGO-containing composites presented larger particles associated with the micrometric lateral size of this kind of filler.

The electrical percolation thresholds in our composites are high as compared with other polymer composites,[48] meaning a poor dispersion of carbon nanoparticles able to reduce the effective particle aspect ratio.[49] Moreover, in copolymers having low crystallinities such as TEPE, the percolation threshold is even higher due to the inverse relationship between the concentration threshold and the matrix crystallinity that is found in similar systems.[50] Hereafter, composites with 8 and 14 wt% of filler were tested regarding their SME as they allowed the analysis of both the percolation transition and type of filler.

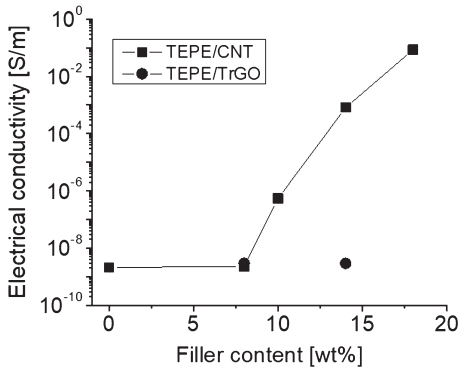

Figure 2. Electrical conductivity of various samples based on TEPE at different filler content.

Double SME

The double SME was analyzed using various programming routes based on the thermal properties of the TEPE matrix having a melting temperature of 37 °C and a glass transition temperature of −57 °C. The shape recovery ratio of the samples was used as defined elsewhere (Eqn (1)).[3] In our particular case, double shape memory was evaluated in a sample having a U-like temporary shape with an angle of 90° and a flat permanent shape with an angle of 180°. Figure 4 displays the shape recovery ratio of samples programed using the melting transition of the matrix meaning: (i) the sample in the permanent shape is strained to a U-like shape and located in an oven at 60 °C for 10 min; (ii) the U-like sample is quenched in a liquid nitrogen bath (around −190 °C) for 10 min; (iii) the sample in the mold is left at room temperature for a couple of days for annealing; and (iv) the sample removed from the mold is located in an oven at 60 °C and the recovery angle is measured. The first conclusion from these data is that pure TEPE matrix without any chemical crosslinking process presented a relevant SME triggered by the melting process. This confirms previous results stating that the presence of hard (bundled crystals in TEPE) and soft (amorphous phase in TEPE) segments is needed to produce SMPs. As the sample was programmed at a temperature above the melting transition, the physical crosslinking in the amorphous state explained the structure able to be strained at this temperature. The bundled crystals formed during cooling switch the temporary shape storing the strain energy coming from the U-like shape. When these crystals melt, this energy is released producing the shape recovery.

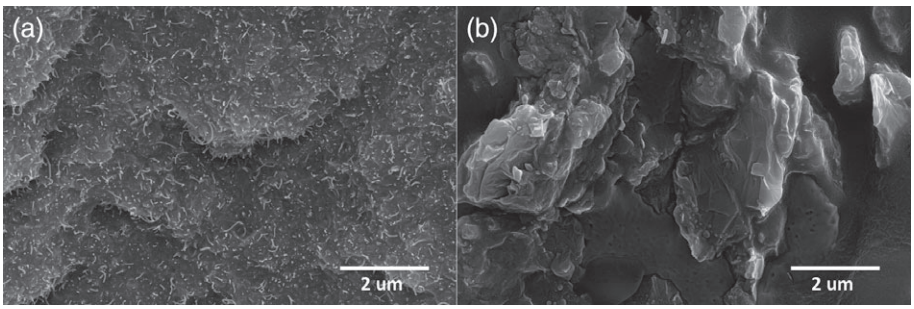

Figure 3. SEM images of some representative composites filled with (a) CNTs and (b) TrGO.

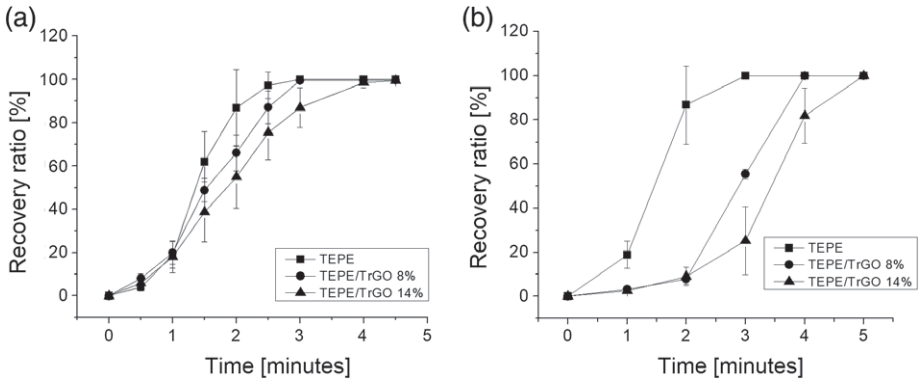

Figure 4. Effect of time on recovery of various TEPE composites switched by melting process by putting the sample in an oven at 60 °C: (a) composites based on CNTs; (b) composites based on TrGO.

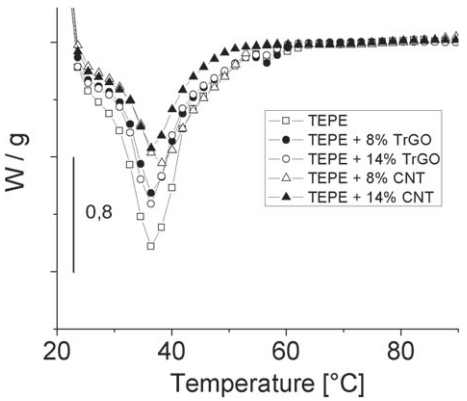

Figure 5. DSC analysis of composites used for SME. Results for the pure polymer (TEPE) are also displayed for comparison.

Figure 4 further shows that this recovery process is delayed in composites with TrGO fillers needing the longest times to reach 100%. The effect of filler on the SME in polymer nanocomposites is a complex issue as the presence of nanoparticles can affect simultaneously both the polymer morphology and its stiffness. In general, by adding nanoparticles the modulus of the resulting composites is increased and therefore more energy is stored by applying a strain (area under stress–strain curve) as compared with pure matrix. By switching the recovery, this higher energy stored in the composite is released explaining the improvement in SME.[34,51] However, the opposite tendency can also be found, with nanoparticles decreasing the strain recovery because of interactions between the nanofiller and the matrix affecting the polymer morphology.[5] For instance, in chemically crosslinked TEPE composite SMPs, the presence of a carbon black network has a deleterious effect on the recovery process.[36] Filler aspect ratio, size and dispersion are relevant variables affecting the crystallization process of the polymer matrix and therefore the SME.[52] Therefore, filler dispersion and changes in polymer morphology are the most relevant variables affecting the SME in polymer composites.[34,52] In our case, TrGO fillers, presenting a high agglomeration degree as concluded from Figs 1–3, render the largest delay in the recovery process supporting the relevance of particle agglomeration in SME. To understand this behavior, DSC was carried out with the samples having the same thermal treatment: quenched from the melt to liquid nitrogen and afterwards annealed at room temperature, as displayed in Fig. 5. These results confirmed that under this thermal treatment carbon nanoparticles affected the crystallinity of the polymer depending on the filler (measured as the area under the heat flow curve divided by the enthalpy of a perfect PE crystal). While CNTs reduced the crystallinity by around 50%, TrGO decreased this property by around 30% due to the low dispersion. These changes in crystallinity relate to the reduction of polymer mobility in the presence of nanoparticles. Similar TEPE polymers mixed with CNTs presented a marked increase in the elastic modulus at low strain frequencies during oscillatory melt experiments.[53] This increase in the elastic behavior can be of several orders of magnitude and it is found near the electrical percolation transition of the composites. In polymer nanocomposites, this rheological transition is due to particle–particle interactions creating a space-filling network able to block the viscous flow of macromolecules.[54] Polymers in these confined spaces crystallize as similar to thin film systems and the formation of lamellae is restricted resulting in a decrease in the degree of crystallinity.[55] Based on these results, a change in polymer morphology arising from a reduction of chain mobility can further explain the delay process by nanofillers. Less crystalline phases produced fewer

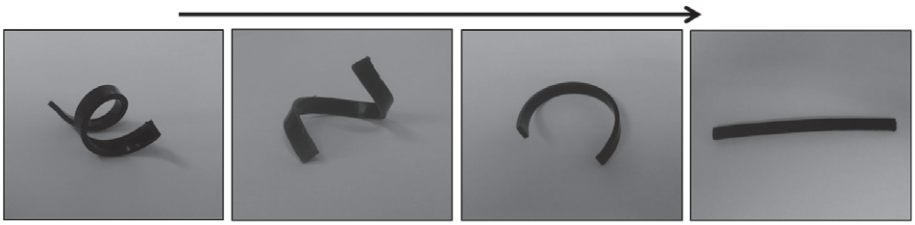

Figure 6. Example of double SME in TEPE composite with 14 wt% of CNTs programed by melting at 60 °C and triggered at the same temperature by putting the sample at an oven. The sample is completely recovered after 8 min.

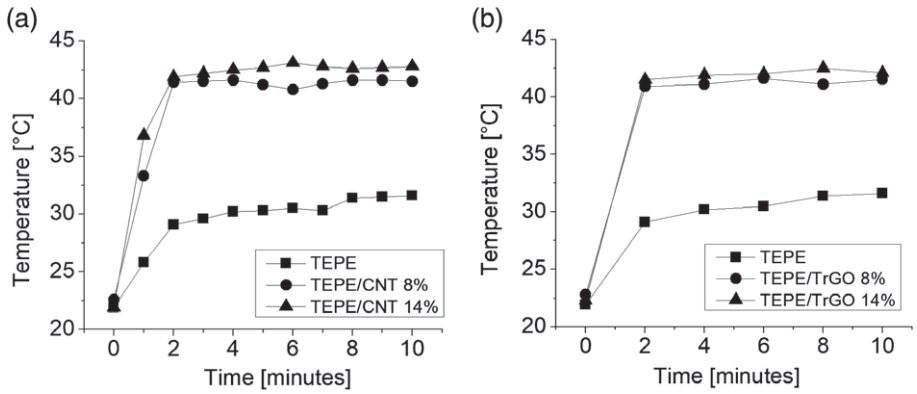

Figure 7. Effect of time and filler concentration on sample temperature under simulated solar radiation: (a) TEPE samples with CNTs; (b) TEPE samples with TrGO.

segments able to switch the temporary shape after thermal treatment, reducing therefore the energy stored. Moreover, the lower mobility produced a delay in the relaxation processes as observed in our SME results. Finally, Fig. 6 shows an example of the SME in a TEPE/CNT composite triggered by thermal transition using a more complex morphology.

Motivated by the melting temperature of TEPE (37 °C), we investigated the SME of the pure matrix under simulated solar radiation of 1 Sun. Figure 7(a) shows the temperature of TEPE under this radiation showing that the surface temperature reached values of around 30 °C after 2 min of exposure. This temperature was lower than the TEPE melting temperature, but the sample was able to present SME as displayed in Fig. 6 associated with the melting of small crystals having transition temperatures of around 30 °C. By comparing these results with Fig. 4, it is concluded that SME under solar radiation is slower by a factor of two than under standard thermal switching because of thermal transfer differences. Noteworthy, by adding carbon nanoparticles to the polymer matrix, the sample temperature was higher, reaching values of around 43 °C under this solar radiation (Fig. 7). It is well known that polymers filled with carbon nanoparticles are able to absorb radiation, mainly infrared light. For instance, the absorption spectrum of a polymer/carbon nanocomposite is not only of wider range but also its absorption is higher than that of the pure polymer.[51] For CNTs, non-radiative decay of infrared photons absorbed raises the internal temperature of the sample.[34] Our results confirmed this tendency, further showing that TEPE nanocomposites presented faster SME than pure matrix (Fig. 8). CNT filler rendered faster behavior than TrGO filler due to the improved dispersion.

Shape memory composites for solar radiation sensor

Electrically conductive SMP composites could be used as sensors or actuators taking advantage of the relationship between deformation and electrical conductivity. Thereby, while the sample is recovering its permanent shape by an appropriate stimulus, the change in the electrical conduction can be monitored.[3] Following the results in Fig. 6, TEPE/CNT composites were studied as sensors for solar radiation by following changes in their electrical resistivity while recovering their permanent shape under this remote stimulus. Indeed, these TEPE/carbon nanocomposites were used as piezoresistive sensors under tensile strain tests.[38] Figure 9 displays the electrical resistivity of TEPE/CNT composite with 14 wt% of filler, relative to the switched state, as a function of the shape memory recovery activated by solar radiation. As the sample recovers its original permanent shape, the electrical resistivity decreases. Percolated polymer/CNT composites under strain, for instance in a programmed U-like shape, presented a decrease in the electrical conductivity due to the filler alignment increasing the interparticle distance and disrupting the particle network.[56] This aligned CNT configuration out of equilibrium is switched by cooling the sample below the melting point producing a temporary state with interparticle CNT distances larger than in the unstrained state. By melting the sample, the strain is released and the CNTs can return to the equilibrium state associated with shorter interparticle distances and therefore higher electrical conductivity. Figure 9 confirms that the SME in TEPE/CNT composites can be triggered remotely by solar radiation producing a change in the electrical conductivity, and therefore they can be used as solar radiation sensors/actuators.

Triple SME

The SME discussed above was triggered by a melting process as the temporary shape was produced in the melt state. However, to obtain a triple SME, another switching mechanism should be defined. In our case, the new switch was associated with the thermal performance of the TEPE amorphous phase having a glass transition at around −57 °C. To validate this procedure, a double shape memory effect was first investigated. The program in this

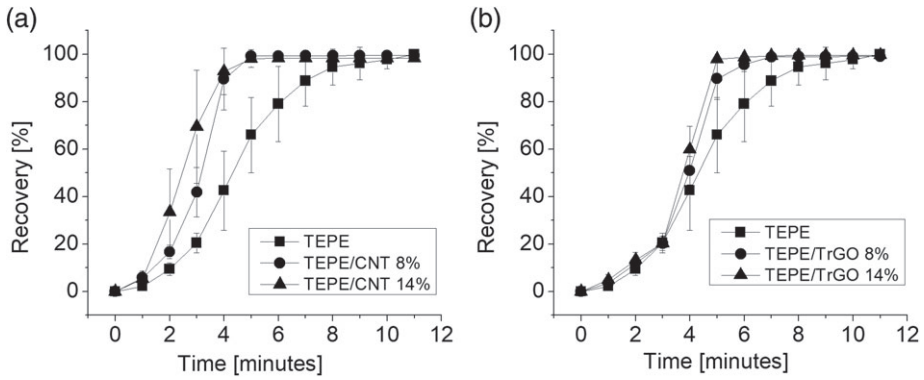

Figure 8. Effect of time on recovery of various TEPE composites switched by melting process by putting the sample under solar radiation: (a) composites based on CNTs; (b) composites based on TrGO.

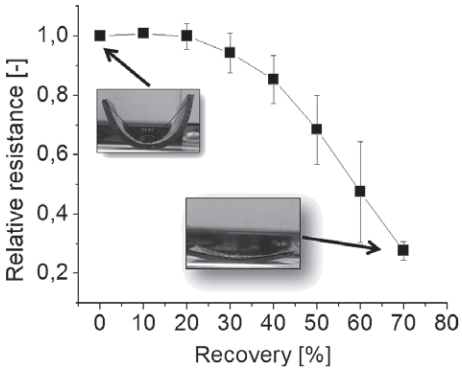

Figure 9. Effect of recovery triggered by solar radiation on electrical behavior of TEPE/CNT composite with 14 wt% of filler. The relative resistance is defined as the ratio between the electrical resistance of the sample in a specific recovery state and the electrical resistance of the original switched sample.

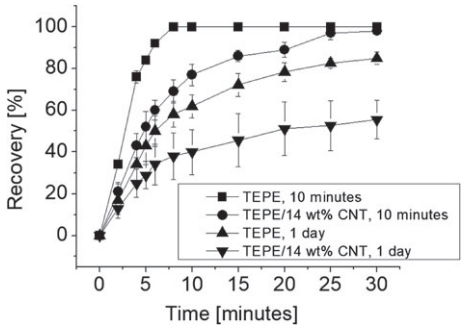

Figure 10. Effect of time on recovery of various TEPE composites switched by glass transition by putting the sample at room temperature after quenching at −190 °C. Two cases were analyzed regarding the time used for room temperature programing (temporary shape): 10 min and 1 day.

case was: (i) the sample is strained to a U-like shape at room temperature for either 10 min or 1 day; (ii) the U-like constrained sample is quenched to −190 °C in 10 min; and (iii) the sample is heated at room temperature for recovery measurements. Figure 10 displays the recovery of TEPE and TEPE/CNT composite with 14 wt% of filler showing SME by this switching mechanism. Pure TEPE was able to recover 100% of the permanent shape at room temperature after a programing process of 10 min. Similar to the SME switched by the melting process, CNTs delay the SME as compared with pure polymer. These results confirm that TEPE can be programed using both melting temperature and glass transition. Noteworthy, the SME depended on the programing time associated with the strained sample at room temperature. While samples programed during 10 min presented complete recovery, samples programed during 1 day were not able to relax completely and the recovery was much lower. This result confirms the relevance of the equilibrium state to the SME as samples reaching equilibrium during long-time programing were not able to store the same energy as compared with samples strained and quenched out of equilibrium.

Based on our results regarding the possibility of switching the TEPE by either melt process (Fig. 4) or glass transition (Fig. 10), a triple SMP was investigated. In this case, the program, as displayed in Fig. 11, was: (i) the sample is strained to a U-like shape at 60 °C for 10 min; (ii) afterwards the sample is cooled to room temperature where an extra strain is carried out; and (iii) the sample is quenched in a liquid nitrogen bath (around −190 °C) for 10 min. The first thermal activation was at room temperature taking advantage of the switch mechanism based on the glass transition. Figure 12 displays the recovery of the TEPE and its composite with 14 wt% of CNTs, showing a complete recovery after 8 and 22 min, respectively, confirming the relevance of CNTs for delaying the SME. Noteworthy, when the sample reached 100% recovery at room temperature, it was located in an oven at 60 °C triggering the second thermal activation based on melting. Both samples reached a 100% recovery (200% in Fig. 12). Therefore, TEPE samples were able to present a triple SME.

CONCLUSIONS

TEPE and its composites with CNTs and TrGO were used as SMPs under various programing conditions. The samples were able to be switched by either melting or glass transition processes allowing double and triple SMEs without the need of a chemical crosslinking process. The addition of carbon nanoparticles to the TEPE matrix delayed the recovery process although all the samples presented 100% recovery. Noteworthy, solar radiation was able to trigger the SME and the composite with 14 wt% of CNTs presented a faster recovery as compared with pure matrix. The percolated TEPE/CNT composite with 14 wt% of filler presented a change in the electrical resistivity during the recovery process under solar radiation allowing the development of multifunctional sensors.

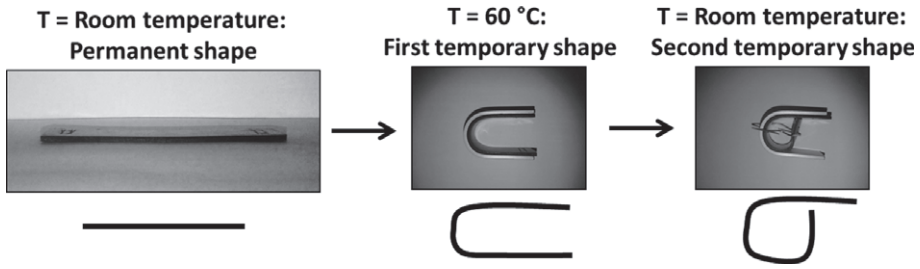

Figure 11. Programing details for a triple SMP based on TEPE and its composite with 14 wt% of CNTs.

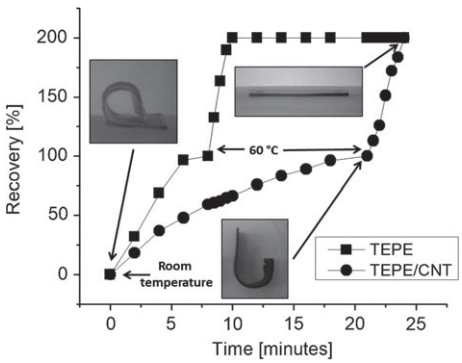

Figure 12. Effect of time on recovery of a triple SMP based on TEPE and its composite with 14 wt% of CNTs. The first recovery was triggered by the glass transition process at room temperature reaching a value of 100%. When the sample reached 100% recovery under this first process, it was located in an oven at 60 °C triggering the second process by melting.

ACKNOWLEDGEMENTS

The authors gratefully acknowledge the financial support of CONICYT under FONDECYT Project 1150130 and FONDEQUIP EQM150101.

REFERENCES

1 Meng Q and Hu J, *Composites A* **40**:1661–1672 (2009).
2 Behl M and Lendlein A, *Mater Today* **10**:20–28 (2007).
3 Leng J, Lan X, Liu Y and Du S, *Prog Mater Sci* **56**:1077–1135 (2011).
4 Behl M, Razzaq MY and Lendlein A, *Adv Mater* **22**:3388–3410 (2010).
5 Ratna D and Karger-Kocsis J, *J Mater Sci* **43**:254–269 (2008).
6 Rousseau IA, *Polym Eng Sci* **48**:2075–2089 (2008).
7 Lin JR and Chen LW, *J Appl Polym Sci* **69**:1563–1574 (1998).
8 Lee BS, Chun BC, Chung YC, Sul KI and Cho WJ, *Macromolecules* **34**:6431–6437 (2001).
9 Li FK, Hou JN, Zhu W, Zhang X, Xu M, Luo XL *et al.*, *J Appl Polym Sci* **62**:631–638 (1996).
10 Wang M and Zhang L, *J Polym Sci B* **37**:101–112 (1999).
11 Wang M, Luo X, Zhang X and Ma D, *Polym Adv Technol* **8**:136–139 (1997).
12 Sakurai K, Shirakawa Y, Kashiwagi T and Takahashi T, *Polymer* **35**:4238–4239 (1994).
13 Li F, Chen Y, Zhu W, Zhang X and Xu M, *Polymer* **39**:6929–6934 (1998).
14 Behl M, Ridder U, Feng Y, Kelch S and Lendlein A, *Soft Matter* **5**:676–684 (2009).
15 Xie T, *Nature* **464**:267–270 (2010).
16 Morshedian J, Khonakdar HA, Mhrabzadeh M and Eslami H, *Adv Polym Technol* **22**:112–119 (2003).
17 Zhu G, Liang G, Xu Q and Yu Q, *J Appl Polym Sci* **90**:1589–1595 (2003).
18 Zheng X, Zhou S, Li X and Weng J, *Biomaterials* **27**:4288–4295 (2006).
19 Jing Z, Shi X, Zhang G, Li J, Li J, Zhou L *et al.*, *Polymer* **92**:210–221 (2016).
20 Liu T, Huang R, Qi X, Dong P and Fu Q, *Polymer* **114**:28–35 (2017).
21 Lendlein A and Langer R, *Science* **296**:1673–1676 (2002).
22 Sauter DW, Taoufik M and Boisson C, *Polymers* **9**:185 (2017).
23 Lendlein A and Kelch S, *Angew Chem Int Ed* **41**:2034–2057 (2002).
24 Maksimkin A, Kaloshkin S, Zadorozhnyy M and Tcherdyntsev V, *J Alloys Compd* **586**:S214–S217 (2014).
25 Kolesov IS, Kratz K, Lendlein A and Radusch HJ, *Polymer* **50**:5490–5498 (2009).
26 Kolesov IS and Radusch HJ, *eXPRESS Polym Lett* **2**:461–473 (2008).
27 Zhao J, Chen M, Wang X, Zhao X, Wang Z, Dang ZM *et al.*, *ACS Appl Mater Interfaces* **5**:5550–5556 (2013).
28 Hoeher R, Raidt T, Krumm C, Meuris M, Katzenberg F and Tiller JC, *Macromol Chem Phys* **214**:2725–2732 (2013).
29 Hoeher R, Raidt T, Rose M, Katzenberg F and Tiller JC, *J Polym Sci B: Polym Phys* **51**:1033–1040 (2013).
30 Bensason S, Minick J, Moet A, Chum S, Hiltner A and Baer E, *J Polym Sci B* **34**:1301–1315 (1996).
31 Yu K, Zhang ZC, Liu YJ and Leng JS, *Appl Phys Lett* **98**:074102 (2011).
32 Cho JW, Kim JW, Jung YC and Goo NS, *Macromol Rapid Commun* **26**:412–416 (2005).
33 Paik IH, Goo NS, Jung YC and Cho JW, *J Mater Sci* **45**:5851–5859 (2010).
34 Koerner H, Price G, Pearce NA, Alexander M and Vaia RA, *Nat Mater* **3**:115–120 (2004).
35 Ahir SV and Terentjev EM, *Nat Mater* **4**:491–495 (2005).
36 Le HH, Kolesov I, Ali Z, Uthardt M, Osazuwa O, Ilisch S *et al.*, *J Mater Sci* **45**:5851–5859 (2010).
37 Le HH, Schoß M, Ilisch S, Gohs U, Heinrich G, Pham T *et al.*, *Polymer* **52**:5858–5866 (2011).
38 Palza H, Garzon C and Rojas M, *Polym Int* **65**:1441–1448 (2016).
39 Garzon C and Palza H, *Compos Sci Technol* **99**:117–123 (2014).
40 Pham GT, Park YB, Liang Z, Zhang C and Wang B, *Composites* **39**:209–216 (2008).
41 Flandin L, Hiltner A and Baer E, *Polymer* **42**:827–838 (2001).
42 Kim H, Miura Y and Macosko CW, *Chem Mater* **22**:3441–3450 (2010).
43 Zhao X, Zhang Q and Chen D, *Macromolecules* **43**:2357–2363 (2010).
44 Cai D, Yusoh K, Song M. *Nanotechnology* **20**:085712 (2009).
45 Palza H, Rojas M, Cortez E, Palma R and Zapata P, *Composites B* **107**:97–105 (2016).
46 Khan U, May P, O'Neill A and Coleman JN, *Carbon* **48**:4035–4041 (2010).
47 Linares A, Canalda JC, Cagiao ME, Garcia-Gutierrez MC, Nogales A, Martin-Gullon I *et al.*, *Macromolecules* **41**:7090–7097 (2008).
48 Bauhofer W and Kovacs J, *Z Comp Sci Technol* **69**:1486–1498 (2009).
49 Micusik M, Omastova M, Krupa I, Prokes J, Pissis P, Logakis E *et al.*, *J Appl Polym Sci* **113**:2536–2551 (2009).
50 Li YJ, Xu M, Feng JQ, Cao XL, Yu YF and Dang ZM, *J Appl Polym Sci* **106**:3359–3365 (2007).
51 Leng J, Wu X and Liu Y, *J Appl Polym Sci* **114**:2455–2460 (2009).
52 Gunes IS, Cao F and Jana SC, *Polymer* **49**:2223–2234 (2008).
53 Palza H, Reznik B, Kappes M, Hennrich F, Naue IFC and Wilhelm M, *Polymer* **51**:3753–3761 (2010).
54 Dorigato A, Pegoretti A and Penati A, *eXPRESS Polym Lett* **4**:115–129 (2010).
55 Khan J, Harton SE, Akcora P, Benicewicz BC and Kumar SK, *Macromolecules* **42**:5741–5744 (2009).
56 Alig I, Lellinger D, Dudkin SM and Pötschke P, *Polymer* **48**:1020–1029 (2007).

